PERGAMON

International Journal of Heat and Mass Transfer 43 (2000) 1885–1896

International Journal of HEAT and MASS TRANSFER

www.elsevier.com/locate/ijhmt

Subcooled flow boiling heat transfer of R-134a and bubble characteristics in a horizontal annular duct

Chih-Ping Yin[a], Yi-Yie Yan[a], Tsing-Fa Lin[a,*], Bing-Chwen Yang[b]

[a]*Department of Mechanical Engineering, National Chiao Tung University, 1001 Ta Hsueh Road, Hsinchu 30010, Taiwan*
[b]*Energy and Resources Laboratories, Industrial Technology Research Institute, Hsinchu, Taiwan*

Received 8 June 1999; received in revised form 6 September 1999

Abstract

Experiments were carried out to investigate the subcooled flow boiling heat transfer and visualize the associated bubble characteristics for refrigerant R-134a flowing in a horizontal annular duct having inside diameter of 6.35 mm and outside diameter of 16.66 mm. The effects of the imposed wall heat flux, mass flux, liquid subcooling and saturation temperature of R-134a on the resulting nucleate boiling heat transfer and bubble characteristics were examined in detail. In the experiment significant hysteresis was noted in the boiling curves during the onset of nucleate boiling (ONB) especially at low saturation temperature and high subcooling. The temperature undershoot at ONB is rather large for most cases. The boiling heat transfer was slightly higher for a lower saturation temperature and was little affected by the mass flux. However, for a higher subcooling of the refrigerant better heat transfer results. Furthermore, the flow visualization revealed that at higher imposed wall heat flux the heated surface was covered with more bubbles and the bubble generation frequency is higher. But the size of the bubbles departing from the heated surface was only slightly affected by the imposed heat flux. At high mass flux and subcooling the bubble generation was suppressed to a noticeable degree. Besides, the bubbles are much smaller at a higher subcooling. Finally, empirical correlations for the heat transfer coefficient and bubble departure diameter in the subcooled flow boiling of R-134a were proposed.

1. Introduction

In view of the quick destruction of the ozone layer in the outer atmosphere around the earth the production of certain CFC and HCFC refrigerants was prohibited recently or will be limited in the near future. New types of refrigerants with zero ozone-depleting potential such as HFC and HC refrigerants have been developed and some are widely used. The heat transfer and pressure drop data for boiling, evaporation and condensation of these new refrigerants are desired to facilitate the design of various air conditioning and refrigeration systems. Recently, efforts had been made by a number of research groups to establish the design database for some new refrigerants for different enhanced surfaces. Moreover, R-134a is currently considered to be the main replacement to many CFC and HCFC refrigerants. In the present study the subcooled flow boiling of R-134a in an annular duct was experimentally investigated by measuring the boiling curves and visualizing the bubbles on the heated surface.

An updated comprehensive review of the literature on boiling of new refrigerants was recently con-

* Corresponding author. Tel.: +886-3-7712-121; fax: +886-3-5720-634.
E-mail address: u8614812@cc.nctu.edu.tw (T.-F. Lin).

0017-9310/00/$ - see front matter
PII: S0017-9310(99)00278-1

Nomenclature

Bo	boiling number ($= q''_w/Gi_{fg}$)
d_p	bubble departure diameter, m
D_h	hydraulic diameter ($= D_o - D_i$), m
D_i	inner heated pipe outside diameter, m
D_o	outer Pyrex inside diameter, m
g	gravitational acceleration, m/s^2
G	mass flux, kg/m^2 s
h_f	specific enthalpy of liquid at saturation temperature, J/kg
h_i	specific enthalpy of subcooled liquid at inlet, J/kg
h_l	all-liquid nonboiling heat transfer coefficient, W/m^2 °C
h_r	boiling heat transfer coefficient, W/m^2 °C
i_{fg}	latent heat of vaporization at saturation temperature, J/kg
k	thermal conductivity, W/m °C
L	length of heated pipe, m
N_{sub}	subcooling number $[= (\frac{h_f - h_i}{i_{fg}})(\frac{v_g - v_f}{v_f})]$
P	system pressure, mm Hg
q''_w	imposed wall heat flux, W/m^2
T	temperature, K
u	flow velocity, m/s
v_f	specific volume of liquid, m^3/kg
v_g	specific volume of vapor, m^3/kg

Greek symbols

ΔT_{sat}	wall superheat ($= T_w - T_{sat}$), °C
ΔT_{sub}	subcooling ($(= T_{sat} - T_f)$, °C
β	dynamic contact angle (°)
ρ	density, kg/m^3
μ	viscosity, Ns/m^2
σ	surface tension, N/m

Subscripts

f	liquid
g	vapor
i	inlet/ inner
r	refrigerant
sat	saturated
sub	subcooling
w	heated wall

ducted by Thome [1]. In the following the relevant literature on the present study is briefly reviewed.

In the past few decades some studies were reported in the literature on the subcooled flow boiling of water and the associated bubble departure size. Gunther [2] performed a photographic study of boiling in a rectangular channel with a heated strip in the middle of the channel for the liquid subcooling ranging from 15 to 65°C, mean flow speed from 1.5 to 12.2 m/s and pressure from 1 to 11 bars. He found that at high subcooling ($\Delta T_{sub} > 38°C$) bubbles were hemispherical which grew and then collapsed while sliding along the heater but did not detach from the heated wall. He also noted that the bubble sliding velocity was approximately 80% of the mean flow velocity. In a heated annulus McAdams et al. [3] reported that the moving of the bubbles into the liquid core caused violent agitation of the liquid near the heated surface and enhanced the heat transfer rate. Recently, Bibeau and Salcudean [4] visualized the bubble cycling in a vertical annular pipe with a high speed photography. They observed that the maximum bubble diameter varied between 0.8 and 3.0 mm and at ejection the bubbles were smaller than the largest bubbles in the liquid, since the ejecting bubbles slided and condensed on the heated wall.

Some studies also exist in the literature on the subcooled flow boiling of refrigerants. Hasan et al. [5] measured the subcooled flow boiling of R-113 in a vertical annular channel with an electrical heated inner pipe and an outer Pyrex glass pipe. They found that the boiling heat transfer coefficient based on the imposed heat flux divided by the difference of the wall temperature and time averaged mixed-mean temperature of the liquid was lower for a higher pressure and for a higher subcooling. Moreover, for a higher mass flux the boiling heat transfer coefficient was mildly lower. Their data agreed well with some correlations [6,7] but showed poor agreement with the modified Chen correlation [8]. Subcooled flow boiling of R-11, R-123 and two R-123/alkybenzene lubricant mixtures in a horizontal circular quartz pipe was investigated by Kedzierski [9]. The pipe was heated by a brass strip of 3 mm wide and 0.25 mm thick placed horizontally along the pipe bottom with its length aligned with the flow direction. He noted that the boiling heat transfer coefficient of R-123 was about 22% higher than R-11 because the boiling in R-123 had approximately 10 more active nucleation sites/cm^2. Moreover, adding a small amount of lubricant into R-123 was found to produce a significant number of new and active nucleation sites and hence can enhance the boiling heat transfer. But a further addition of the lubricant resulted in an opposite trend. Furthermore, he found that the bubble diameter was independent of the Reynolds number of the mean flow and the imposed heat flux. The measured bubble diameter was in good agreement

with the Fritz equation [10]. Klausner et al. [11] measured the bubble departure diameter for the saturated flow boiling of R-113 in a rectangular channel with an electrically heated nichrone plate of 20 mm wide and 0.127 mm thick on the channel bottom. They found that the bubble departure diameter is smaller for a higher mass flow rate and for a lower imposed heat flux. They also noted that before lifting off from the heated wall, the bubbles would slide a finite distance along the surface. They concluded that not only the surface tension force but also the asymmetrical bubble growth acting in the direction opposite to the fluid motion were important in holding the bubbles at the nucleation sites before departure.

Subcooled flow boiling heat transfer of heptane on a resistance-heated coiled wire of diameter 1.25 mm contained in a concentric annulus was examined by Muller-Steinhagen et al. [12]. Their results indicated that the boiling heat transfer coefficient increased with increasing heat flux but decreased with increasing system pressure and subcooling, while independent of the mass flux. The hysteresis in the boiling curves was small. Similar study carried out by Bland [13] showed that the hysteresis decreased at a higher flow velocity.

Experimental measurements and empirical correlations for the size of the departure bubbles in the saturated boiling were carried out and proposed by Cole and Shulman [14]. They measured the bubble departure size in various liquids at subatmospheric pressure. Specifically, they obtained data for toluene at 48 mm Hg, acetone at 222 and 461 mm Hg, carbon tetrachloride at 138 mm Hg, *n*-pentane at 524 mm Hg, methanol from 134 to 540 mm Hg and water from 50 to 360 mm Hg. Their results indicated that the Fritz equation [10]

$$d_p = 0.0208\beta\left[\frac{\sigma}{g(\rho_f - \rho_g)}\right]^{1/2} \tag{1}$$

was applicable only at the atmospheric pressure. A modified correlation was proposed in their study as

$$\frac{d_p}{\left[\dfrac{\sigma}{g(\rho_f - \rho_g)}\right]^{1/2}} = \frac{1000}{P} \tag{2}$$

The above literature review clearly indicates that the experimental data for the subcooled flow boiling heat transfer in channels and the associated bubble characteristics for the widely used new refrigerant R-134a are not available. In this study, the subcooled flow boiling of R-134a in an annular duct was explored experimentally. The effects of the imposed heat flux, mass flux, subcooling and saturation temperature (pressure) of R-134a on the subcooled boiling heat transfer characteristics were investigated. Meanwhile, flow visualization was conducted to examine some boiling characteristics such as the distribution of the bubble size and the density of the nucleation sites. Moreover, the hysteresis existing in the subcooled nucleate boiling was inspected.

2. Experimental apparatus and procedures

The experimental apparatus established in the present study to investigate the subcooled boiling of R-134a, schematically shown in Fig. 1, consists of two main loops, namely, the refrigerant and water–glycol loops, and a data acquisition system. Refrigerant R-134a is circulated in the refrigerant loop. We need to control the temperature and flow rate in the water–glycol loop to have enough cooling capacity for condensing the R-134a vapor and subcooling the R-134a liquid to a preset subcooled temperature. A DC power supply is used for heating the inner pipe in the test section. For measuring the bubble size and nucleation density in the R-134a subcooled flow boiling on the heated surface, a camera connected to a photographic microscope is set up beside the test section to observe the boiling flow.

2.1. Refrigerant loop

The refrigerant loop contains a refrigerant pump, an accumulator, a mass flow meter, a test section, a condenser, a sub-cooler, a receiver, a filter/dryer and three sight glasses. A rotational DC motor is used to drive the refrigerant pump. Through changing the DC current in the motor the liquid flow rate of R-134a can be varied. By adjusting the gate opening of the valve at the downstream of the test section, the pressure of the refrigerant in the test section can be regulated. Note that the refrigerant flow rate and the pressure should be further adjusted simultaneously in order to control them at the required levels. Moreover, the accumulator is installed to dampen the fluctuations of the flow rate and pressure. The refrigerant flow rate is measured by a mass flow meter with an accuracy of 1%. Meanwhile, a condenser and a subcooler are used to condense the R-134a vapor leaving the test section and then subcool the liquid R-134a. Varying the temperature and flow rate of the water–glycol mixture moving through the condenser and subcooler allows us to control the bulk temperature of R-134a leaving the subcooler. After subcooled, the liquid R-134a flows back to the receiver.

2.2. Test section

As schematically shown in Fig. 2, the test section is

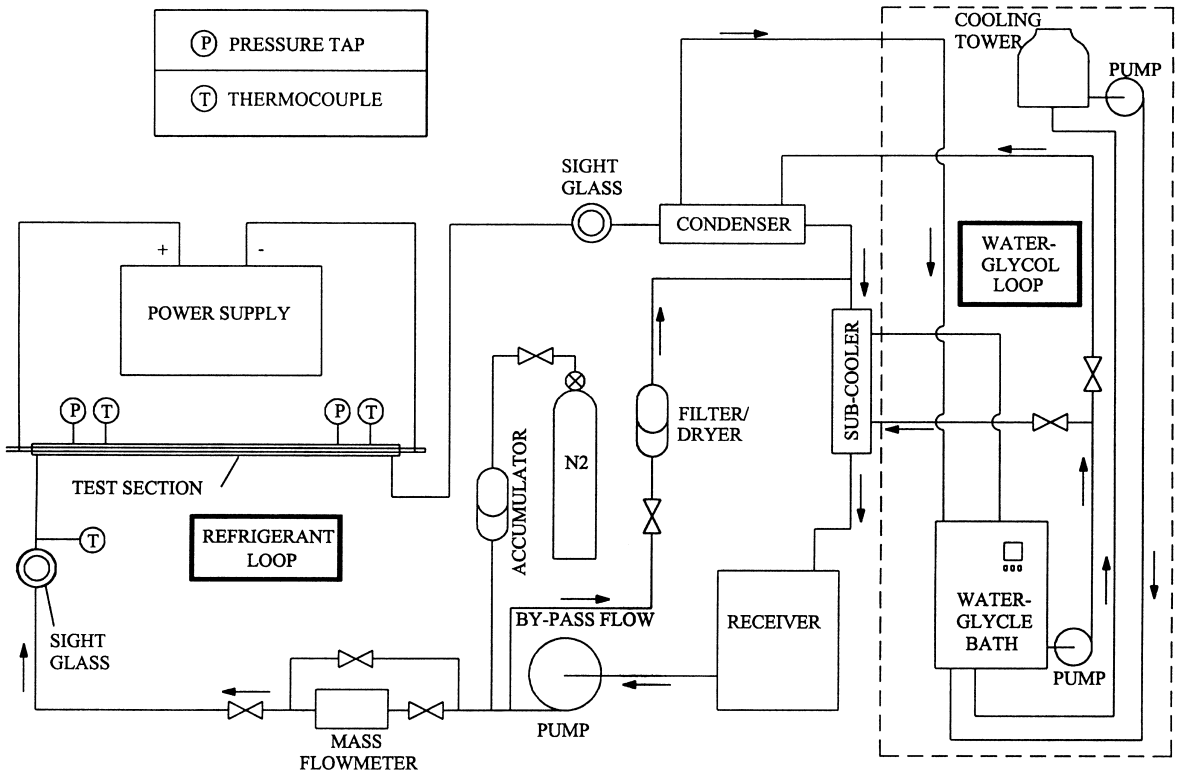

Fig. 1. Schematic diagram of the experimental system.

a horizontal annular duct with the outer pipe made of pyrex glass to facilitate the visualization of boiling processes. The outer pipe has an inside diameter of 16.66 mm and is 4 mm thick. A circular, electrically heated SS-304 inner pipe is used as the heating surface and the subcooled R-134a liquid enters the annular passage flowing over the heating surface. This heated inner pipe has an outside diameter of 6.35 mm and it is 21 cm long and 1 mm thick. This stainless steel pipe was soldered with two pure copper pipes of the same size at their ends. Careful procedures have been taken to insure that these three pipes are connected intactly and

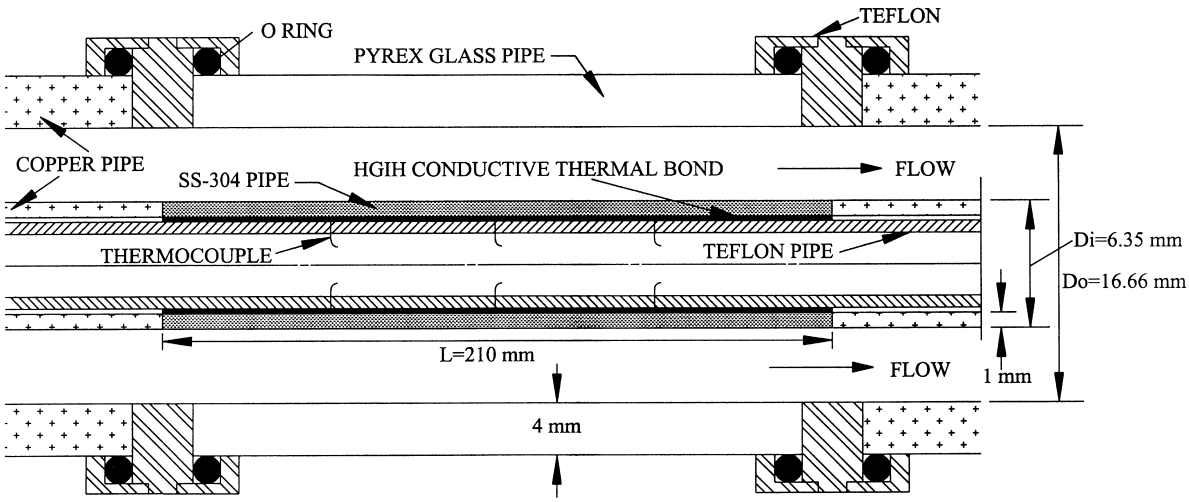

Fig. 2. Schematic diagram of the test section for subcooling boiling.

are like a single straight pipe. The copper pipes allow the DC current to deliver from the power supply to pass through the SS-304 pipe.

To measure the temperature of the heating surface, the inner surface of the SS-304 pipe is covered with a thin high conductivity thermal bond (k = 200 W/m °C), as indicated in Fig. 2. Then 12 T-type thermocouples are fixed onto the thermal bond so that the voltage signals from the thermocouples are not interfered by the DC current passing through the heating surface. The thermocouples are positioned at three axial stations. At each axial station four thermocouples are placed at the top, bottom and two sides of the circumference with 90° apart. Moreover, the thermal bond is further covered by a teflon pipe of 0.3 mm thick to reduce the heat loss from the SS-304 pipe. Note that the temperature of the boiling surface can be evaluated from the thermocouple data.

A DC power supply with a maximum rating of 20 kW provides the electric current passing through first to the copper pipe and then to the stainless steel pipe. The DC current passing through the heating pipe is measured by a Yokogawa DC meter with an accuracy of 1%. Moreover, the voltage drop across the heating pipe is measured by a Yokogawa multimeter and the power input to the heating pipe can then be calculated. The refrigerant R-134a pressure is measured by a pressure transducer with an accuracy of 1%.

2.3. Water–glycol mixture loop

The water–glycol loop designed for condensing the R-134a vapor and for subcooling the liquid R-134a contains a 125-litre constant temperature bath with a water cooled refrigeration system. The cooling capacity is 2 kW for the water–glycol mixture at −20°C. The cold water–glycol mixture at a specified flow rate is driven by a 0.5 hp pump to the condenser as well as to the subcooler. A by-pass loop is provided to adjust the flow rate. By adjusting the mixture temperature and flow rate, the bulk temperature of the R-134a in the subcooler can be controlled at a preset level.

2.4. Data acquisition

The data acquisition system for recording and processing the signals from the thermocouples and pressure transducers includes a recorder and a controller. The recorder is used to record the temperature and voltage data. The IEEE488 interface is used to connect the controller and the recorder, allowing the measured data to transmit from the recorder to the controller and then analyzed by the computer immediately.

2.5. Experimental

In the test the subcooled R-134a liquid at the inlet of the test section is first maintained at a specified subcooling by adjusting the water–glycol temperature and flow rate. Then, we regulate the R-134a pressure at the test section inlet by adjusting the gate opening of the valve locating right after the exit of the test section. Meanwhile, by changing the current of the DC motor connecting to the refrigerant pump, the R-134a flow rate can be adjusted. The imposed heat flux from the heater to the R-134a is adjusted by varying the electric current delivered from the DC power supply. By measuring the current and voltage drop across the heater, we can calculate the amount of the heat transfer rate to the refrigerant.

Generally and also in the present study, the boiling heat transfer coefficient is defined as the average imposed heat flux divided by the wall superheat $T_w - T_{sat}$. For some cases the subcooled flow boiling heat transfer coefficient is defined here as the heat flux divided by the difference of the wall and bulk temperatures, especially when discussing the subcooling effects [5].

2.6. Uncertainty analysis

The uncertainties of the experimental results are analyzed by the procedures proposed by Kline and McClintock [15]. The results from this analysis indicate that the uncertainties associated with the temperature and pressure measurements are respectively 0.3°C and 0.002 MPa. While for the imposed heat flux and mass flux of R-134a the uncertainties are about 3 and 2%, respectively. The uncertainty for the boiling heat transfer coefficient is about 16%. The detailed results from the present uncertainty analysis for the experiments conducted here are summarized in Table 1.

Table 1
Parameters and estimated uncertainties

Parameter	Uncertainty
Length, width and thickness (m)	±0.5%
Area (m^2)	±1%
Temperature, T (°C)	±0.2°C
ΔT (°C)	±0.3°C
Pressure, P (MPa)	±0.002 MPa
Mass flux of refrigerant, G	±2%
Heat flux, q''_w	±3%
Boiling heat transfer coefficient, h_r	±16%

3. Results and discussion

In the present study experiments were conducted for the refrigerant mass flux varying from 100 to 300 kg/m^{2}s, imposed heat flux from 0 to 20 kW/m^2, subcooling from 6 to 13°C and saturation temperature from −6 to 1°C. In what follows selected data are reported to illustrate the characteristics of the subcooled flow boiling heat transfer for R-134a in an annular duct by presenting the nucleate boiling curves for various cases. Effects of the mass flux, heat flux, subcooling and saturation temperature on the heat transfer data will be examined in detail. In addition, the associated bubble characteristics in the subcooled boiling on the heated surface will be inspected based on the results from the flow visualization.

3.1. Boiling curves

Effects of the mass flux on the R-134a subcooled flow boiling heat transfer are manifested first in Figs. 3 and 4 for different subcooling and saturated temperatures. An inspection of a given boiling curve for a fixed mass flux reveals that as the imposed heat flux is raised gradually from an unheated state, the temperature of the heated wall T_w increases slowly. This increase in T_w is almost linear, suggesting that no boiling takes place in the R-134a liquid flow and the heat transfer in the flow is due to single phase forced convection. It is of interest to note that this single phase heat transfer region extends significantly to the wall temperature well above the saturated value T_{sat}. The wall superheat, $T_w - T_{sat}$, can be as high as 18°C for G = 300 kg/m^{2}s in Fig. 3 with $\Delta T_{sub} = 10$ °C and $T_{sat} = -2$°C. It is further noted that at a certain high wall superheat a very small raise of the imposed heat flux causes the heated wall temperature to drop substantially, obviously due to the sudden appearance of the boiling on the wall. Thus, we have onset of nucleate boiling (ONB) at this wall heat flux. This temperature undershoot during ONB is rather significant in the subcooled flow boiling of R-134a according to the present data. Note that at a high liquid subcooling for $\Delta T_{sub} = 10$ °C the temperature undershoot is larger for a high R-134a mass flux (see Fig. 3). But at a lower subcooling for $\Delta T_{sub} = 6$ °C the situation is different (see Fig. 4). More specifically, at the lowest G of 100 kg/m^2 s the temperature undershoot is the largest. While at the higher G of 200 and 300 kg/m^2 s the undershoot is nearly at the same magnitude. In the single phase region the wall heat flux at a given wall superheat is higher for a higher mass flux. This indicates that an increase in the mass flux results in better heat transfer. But in the nucleate boiling region beyond ONB the R-134a mass flux shows negligible effects on the boiling heat transfer from the heated wall. It should be pointed out that when the imposed heat flux is lowered gradually from a high level at which the boiling on the heated wall is rather intense, the nucleate boiling can be maintained at a very low wall superheat. We have boiling even at a wall superheat of 2°C (see Fig. 3). This clearly illustrates the existence of the significant hyteresis in the boiling curves.

Next, the R-134a subcooled flow boiling curves for various saturation temperatures with T_{sat} = −55, −2 and 1°C shown in Fig. 5 for G = 200 kg/m^2 s and

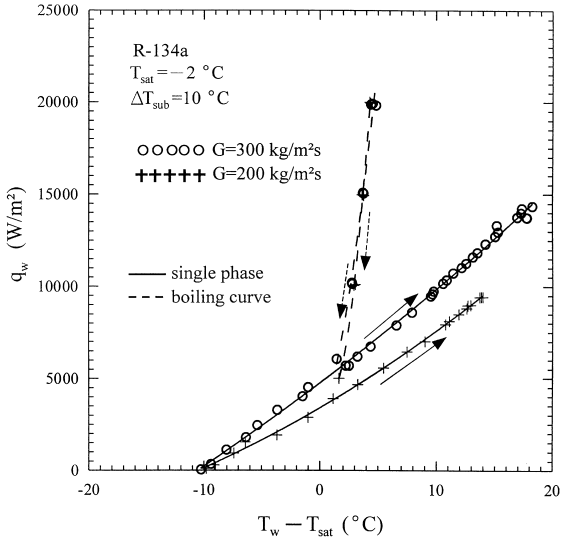

Fig. 3. Comparison of the subcooled flow boiling curves for G = 200 and 300 kg/m^2 s at $T_{sat} = -2$°C and $\Delta T_{sub} = 10$°C.

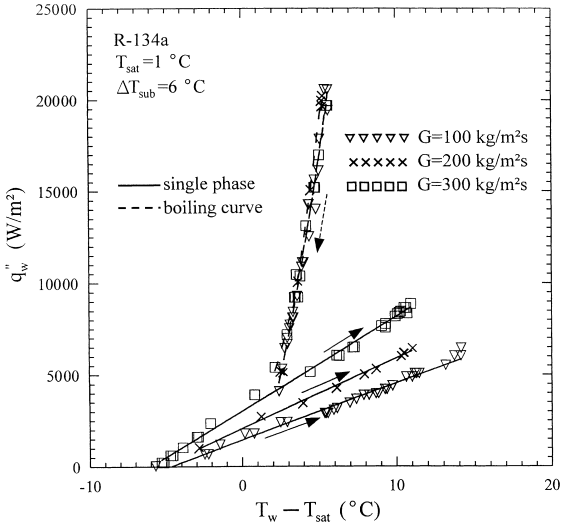

Fig. 4. Comparison of the subcooled flow boiling curves for G = 100, 200 and 300 kg/m^2 s at $T_{sat} = 1$°C and $\Delta T_{sub} = 6$°C.

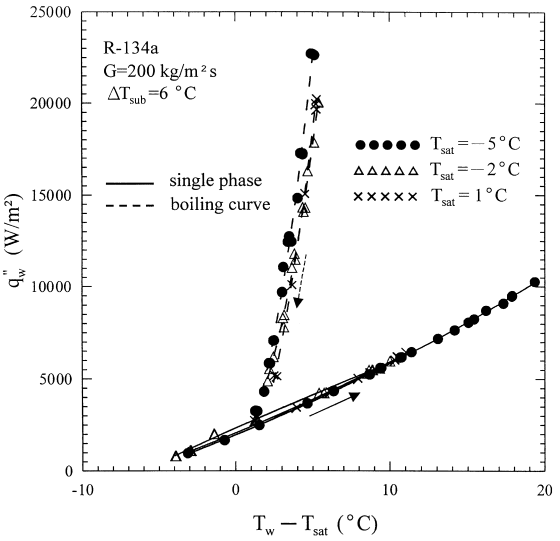

Fig. 5. Comparison of the subcooled flow boiling curves for $T_{sat} = -5$, -2 and 1°C at $G = 200$ kg/m^2 s and $\Delta T_{sub} = 6$°C.

$\Delta T_{sub} = 6$ °C indicate that the temperature undershoot is much larger for the low T_{sat} of -5°C. But for $T_{sat} = -2$ and 1°C the corresponding temperature undershoots are nearly the same. While in the nucleate boiling region the effects of the saturation temperature on the boiling heat transfer is slight. The boiling heat flux for $T_{sat} = -5$°C is only slightly higher than those for $T_{sat} = -2$ and 1°C.

The effects of the subcooling are shown in Fig. 6 for $\Delta T_{sub} = 6$ and 13°C at $G = 200$ kg/m^2 s and $T_{sat} = 1$°C. The results indicate that at a higher subcooling

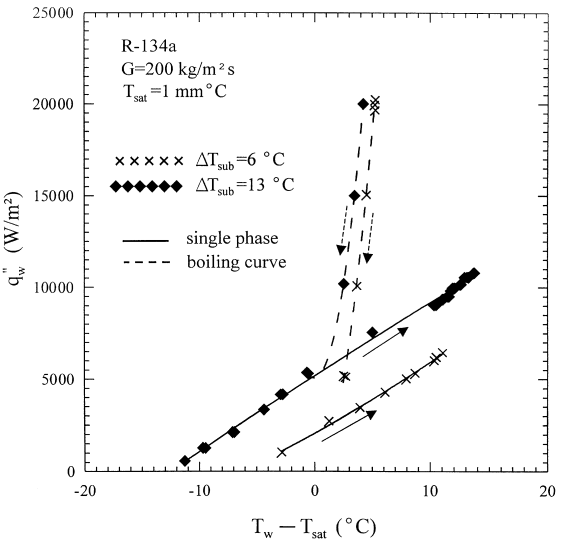

Fig. 6. Comparison of the subcooled flow boiling curves for $\Delta T_{sub} = 6$ and 13°C at $G = 200$ kg/m^2 s and $T_{sat} = 1$°C.

the temperature undershoot is larger. Besides, the single phase and boiling heat transfer is substantially higher for a higher subcooling.

Then, the present data were compared with those evaluated from the Shah correlations [6] for the subcooled flow boiling in annuli. In that study Shah has proposed correlations for saturated and for subcooled flow boiling mainly for water, methanol and R-113. Among which the correlation proposed for the high subcooling is compared with the present data here. His correlation is

$$h_r = h_l\left(230 \cdot Bo^{0.5} + \frac{\Delta T_{sub}}{\Delta T_{sat}}\right) \tag{3}$$

here h_l is the all-liquid nonboiling heat transfer coefficient and is calculated from the McAdams equation as

$$\frac{h_l D_h}{k_f} = 0.023\left(\frac{GD_h}{\mu}\right)^{0.8} Pr^{0.4} \tag{4}$$

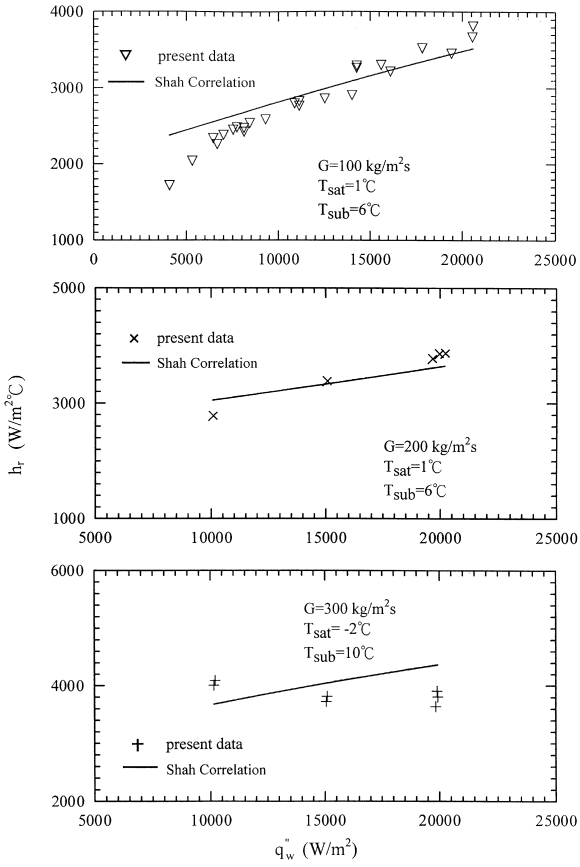

Fig. 7. Comparisons of the present data with the Shah correlation for q''_w from about 5000 to 20 000 W/m^2 at (a) $G = 100$, (b) $G = 200$ and (c) $G = 300$ kg/m^2 s.

Fig. 7 shows the comparison between the present data and Shah correlation. Note that the average deviation is about 16.5%. It should be mentioned that our data for the low subcooling which are not shown here are substantially different from the corresponding correlation values from Shah.

Finally, the present data for heat transfer coefficient in the subcooled flow boiling of R-134a are correlated as

$$h_r = h_l\left[282 \cdot \ln(Bo) + \frac{\Delta T_{sub}}{\Delta T_{sat}} + 27.4\right] \quad (5)$$

The above equation well correlates the present data with an average deviation of 9.9%, as shown in Fig. 8.

3.2. Bubbles in subcooled boiling

It is well known that the effects of various parameters on the R-134a subcooled flow boiling heat transfer presented above have to be related to the characteristics of bubbles on the heated surface during the boiling. These bubble characteristics are examined in the following.

Fig. 9 shows the typical photos of bubbles taken from the present flow visualization for various imposed heat fluxes for $G = 200$ kg/m^2 s, $T_{sat} = -5$°C and $\Delta T_{sub} = 7$ °C. The results indicate that at a higher q''_w a larger fraction of the heated surface is covered by the bubbles. Besides, the bubble generation frequency and bubble rising velocity in the liquid were found to be also higher. Thus, the corresponding boiling heat transfer from the surface is better. A close inspection of the photos reveals that most bubbles are elliptic and the largest bubbles are about 0.6 mm in average diameter, which is rather small in comparison with those in boiling of water. Moreover, the bubbles are largest when they are about to departure from the surface. Note also that the maximum bubble size changes only slightly with the imposed heat flux.

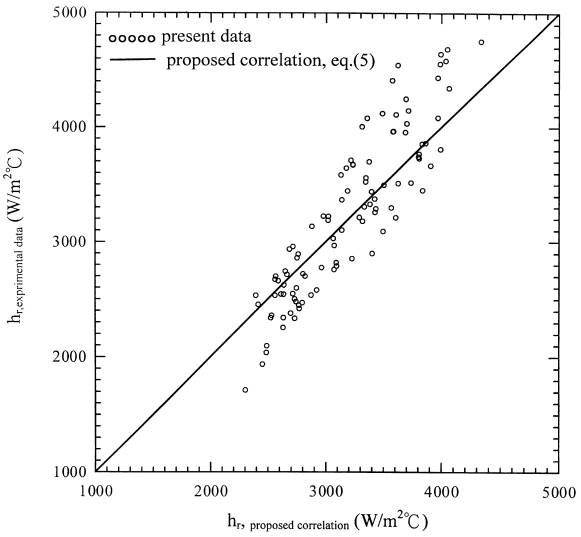

Fig. 8. Comparison of the measured data for heat transfer coefficient in the subcooled flow boiling of R-134a with the proposed correlation.

The results from the visualization of bubbles for various mass fluxes shown in Fig. 10 suggest that at a lower mass flux more bubbles are generated at a larger number of active nucleation sites and at a higher frequency. This mainly attributes to the fact that the heated surface temperature and hence the wall superheat are higher for a lower G. Secondly, the liquid refrigerant R-134a moves faster at a higher G, which tends to sweep the bubbles away from the surface. However, the bubble sizes are not affected by the mass flux to a noticeable degree.

Next, in Fig. 11 we show that the subcooling of the refrigerant exhibits profound influences on the bubble size and population. At the higher subcooling of 13°C the bubbles are much smaller and are in larger number, compared with those for $\Delta T_{sub} = 6$ °C and $\Delta T_{sub} = 0$ °C. This outcome results from the fact that in a highly subcooled liquid the bubbles are significantly suppressed by the surrounding liquid and grow slowly. For example, the bubbles about to depart from the heated surface for $\Delta T_{sub} = 13$ °C have diameter about $d_p \cong 0.3$ mm. But for $\Delta T_{sub} = 6$ °C, $d_p \cong 0.6$ mm and for $\Delta T_{sub} = 1$ °C, $d_p \cong 1.0$ mm. According to the present data, an empirical correlation for the bubble departure diameter modified from that of Cole and Shulman [14] for the saturated flow boiling is proposed here for the subcooled flow boiling of R-134a and it is

$$\frac{d_p}{\left(\frac{\sigma}{g(\rho_f - \rho_g)}\right)}^{1/2} = 2.84 \times \frac{1000}{P}\exp(-0.184N_{sub}) \quad (6)$$

where N_{sub} is the subcooling number, defined as

$$N_{sub} = \left(\frac{h_f - h_i}{i_{fg}}\right)\left(\frac{v_g - v_f}{v_f}\right) \quad (7)$$

The above equation well correlates the present data with an average deviation of 12.6%, as shown in Fig. 12.

4. Concluding remarks

Experiments have been carried out in the present study to investigate the subcooled nucleate flow boiling heat transfer and the associated bubble characteristics

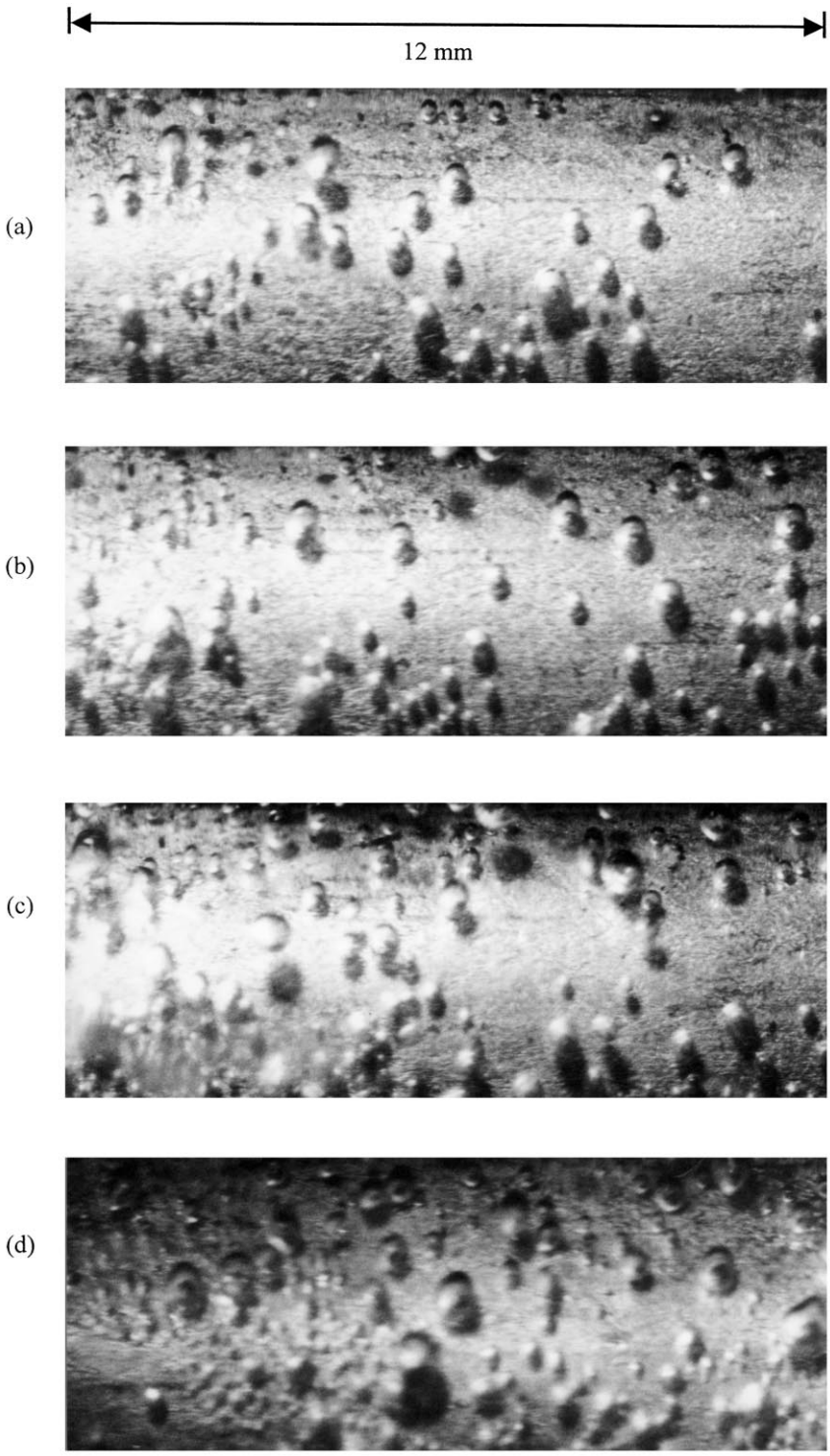

Fig. 9. Subcooled flow boiling of R-134a in an annular channel at $G = 200$ kg/m^2 s $T_{sat} - 5$°C and $\Delta T_{sub} = 7$°C: (a) $q''_w = 5$ kW/m^2 (b) $q''_w = 10$ kW/m^2 (c) $q''_w = 15$ kW/m^2 and (d) $q''_w = 20$ kW/m^2.

for R-134a in an annular duct. Effects of various parameters on the hysteresis during the onset of nucleate boiling (ONB) were examined in detail. At lower T_{sat} and higher ΔT_{sub} the temperature undershoots during ONB are larger. But the mass flux of R-134a shows a nonmonotonic effect on the temperature undershoot. It was noted that the boiling heat transfer is not significantly affected by the mass flux, imposed heat flux and

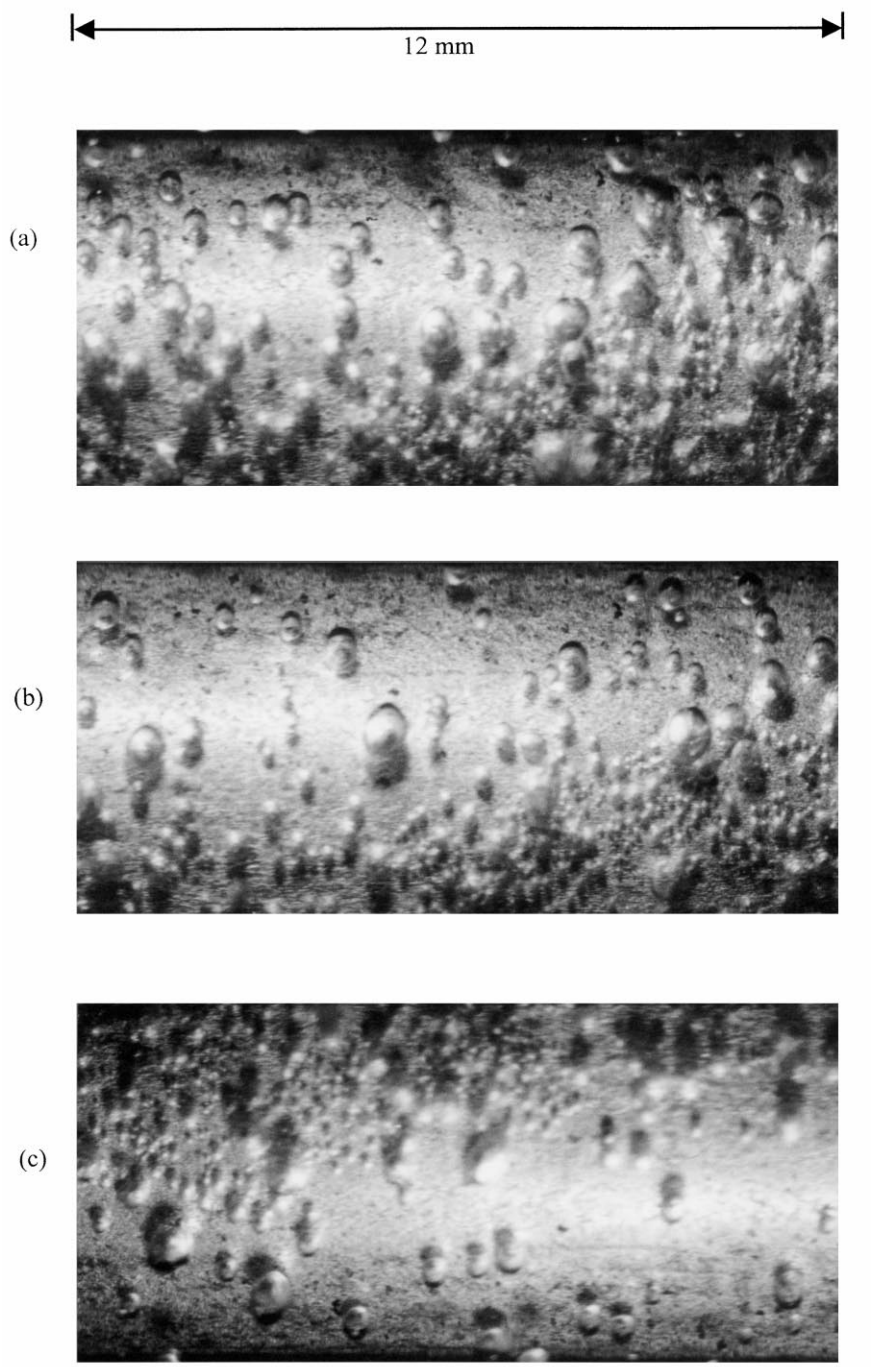

Fig. 10. Subcooled flow boiling of R-134a in an annular channel at $q''_w = 10$ kW/m^2 $T_{sat} = 2.5$°C and $\Delta T_{sub} = 7$°C: (a) $G = 100$ kg/m^2 s, (b) $G = 200$ kg/m^2 s and (c) $G = 300$ kg/m^2 s.

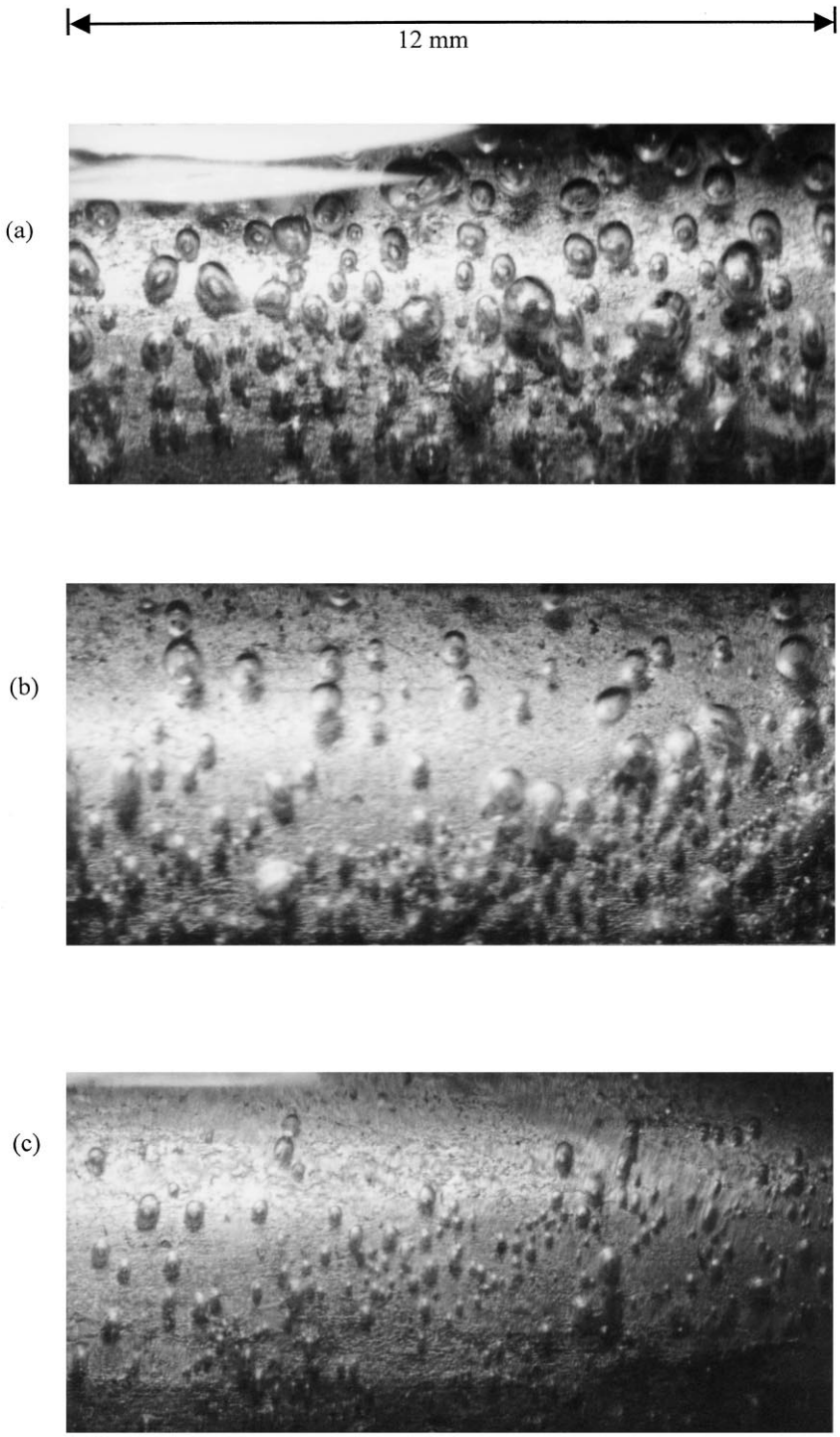

Fig. 11. Subcooled flow boiling of R-134a in an annular channel at $G = 200$ kg/m^2 s, $q''_w = 10$ kW/m^2 and $T_{sat} = 1^\circ$C: (a) $\Delta T_{sub} = 6^\circ$C and (b) $\Delta T_{sub} = 13^\circ$C.

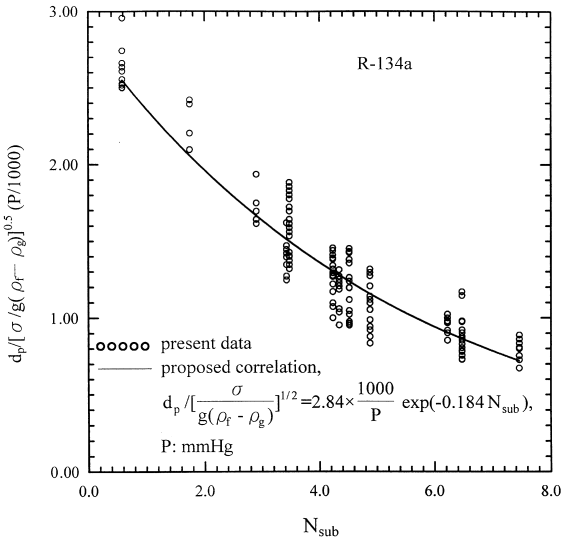

Fig. 12. Comparison of the measured bubble departure diameters with the proposed correlation.

saturation temperature. But an increase in the subcooling results in much better heat transfer. Flow visualization of the boiling processes revealed that the bubble generation frequency was suppressed by raising the mass flux and subcooling of R-134a. Moreover, only the subcooling showed a large effect on the bubble size. Finally, empirical correlations for the boiling heat transfer coefficient and for the bubble departure diameter in the subcooled flow boiling of R-134a based on the present data were provided.

Some other important phenomena such as the influences of the oil contamination on the R-134a flow boiling and condensation characteristics remain largely unknown. This will be explored in the future.

Acknowledgements

The financial support of this study by the engineering division of National Science Council of Taiwan, R.O.C. through the contract NSC85-2221-E-009-046 is greatly appreciated.

References

[1] J.R. Thome, Boiling of new refrigerants: a state-of-the art review, Int. J. Refrig. 19 (1996) 435–457.
[2] F.C. Gunther, Photographic study of surface-boiling heat transfer to water with forced convection, ASME Transaction C Journal of Heat Transfer 73 (1951) 497–499.
[3] W.H. McAdams, W.E. Kennel, C.S. Minden, R. Carl, P.M. Picornell, J.E. Dew, Heat transfer at high rates to water with surface boiling, Indust. Engng. Chem. 41 (1949) 1945–1953.
[4] E.L. Bibeau, M. Salcudean, A study of bubble ebullition in forced-convective subcooled nucleate boiling at low pressure, Int. J. Heat and Mass Transfer 37 (1994) 2245–2259.
[5] A. Hasan, R.P. Roy, S.P. Kalra, Experiments on subcooled flow boiling heat transfer in a vertical annular channel, Int. J. Heat and Mass Transfer 33 (1990) 2285–2293.
[6] M.M. Shah, Generalized prediction of heat transfer during subcooled boiling in annuli, Heat Transfer Engng 4 (1) (1983) 24–31.
[7] K.E. Gunger, R.H.S. Winterton, A general correlation for flow boiling in tubes and annuli, Int. J. Heat and Mass Transfer 29 (1986) 351–358.
[8] J.G. Collier, Convective Boiling and Condensation, McGraw-Hill, New York, 1981, pp. 211–221 (Chapter 7).
[9] M.A. Kedzierski, Simultaneous visual and calorimetric measurements of R11, R123, and R123/alkylbenzene nucleate flow boiling, State of the Art and Emerging Technologies in Enhanced Heat Transfer, A Short Course by the University of Maryland, College of Engineering, April 18/19, 1996.
[10] W. Fritz, Berechnung des Maximalvolumens von Dampfblasen, Physik, Zeitschr 36 (1935) 379–384.
[11] J.F. Klausner, R. Mei, D.M. Bernhard, L.Z. Zeng, Vapor bubble departure in forced convection boiling, Int. J. Heat and Mass Transfer 36 (1993) 651–662.
[12] H. Muller-Steinhagen, A.P. Watkinson, N. Epstein, Subcooled-boiling and convective heat transfer to heptane flowing inside an annulus and past a coiled wire: part 1—experimental results, ASME Transaction C Journal of Heat Transfer 108 (1986) 922–927.
[13] M.E. Bland, Bubble nucleation in cryogenic fluids. Ph.D. thesis, Oxford University, England, 1970.
[14] R. Cole, H.L. Shulman, Bubble departure diameters at subatmospheric pressures, Chemical Engineering Progress, Symposium Series 62 (64) (1996) 6–16.
[15] S.J. Kline, F.A. McClintock, Describing uncertainties in single-sample experiments, Mechanical Engineering 75 (1953) 3–12.